PARTIAL REDISTRIBUTION EFFECTS IN THE FORMATION OF HYDROGEN LINES IN QUIESCENT PROMINENCES

P. Heinzel[1], P. Gouttebroze[2], and J.C. Vial[2]

1. Astronomical Institute of the Czechoslovak Academy of Sciences
25165 Ondrejov, Czechoslovakia

2. Laboratoire de Physique Stellaire et Planétaire
B.P. 10 - F-91371 Verrières-le-Buisson Cédex, France

ABSTRACT

Departures from complete frequency redistribution (CRD) in hydrogen lines are investigated for solar prominences. Partial redistribution effects (PRD) are found both in the wings (their already known lowering) and in the central part of the Lα line; a new feature is evidenced here: the partially coherent scattering in the near wings of the line leads to a double-peaked profile mirroring the incident solar radiation. With a low density model, we obtain a good agreement with OSO 8 observed profiles. On the contrary, the PRD computed Lβ profile (lower density, no reversal) departs from the observed one, a result which calls for more progress in terms of non l.t.e. transfer and modelling.

1. INTRODUCTION

During the last decade, several highly-sophisticated partial-redistribution techniques (PRD) have been applied to the analysis of the strong resonance lines formed in the solar chromosphere, plages or sunspots. Being low-density structures, solar prominences are also very good candidates for possible departures from complete redistribution (CRD), at least for most opaque lines like hydrogen Lα or Lβ.As reported by Vial (1982a), various high-resolution Lα and Lβ line profiles of a quiescent prominence have been recorded by the LPSP spectrometer on board of OSO-8 satellite. Applying the two-dimensional radiative transfer code of Mihalas et al. (1978), Vial (1982b) has simulated theoretical Lα profiles (using a two-level atom and CRD) and made a comparison of their basic parameters with those corresponding to OSO-8 data. The agreement was satisfactory, but no direct comparison between the shapes of the theoretical and measured profiles was presented in this study. It is the aim of the present paper to make possible a first comparison of OSO-8 Lα and Lβ profiles with theoretical PRD computations in order to assess the real importance of departures from CRD. Moreover, we investigate the behaviour of the total CRD and PRD intensities of the hydrogen lines and compare our results with those of Milkey et al. (1979) and with the data presented by Heinzel and Vial (1983).

2. PROMINENCE MODELS

Since our principal interest is to estimate PRD effects on hydrogen lines, we start here with simple one-dimensional (1D) isothermal-isobaric prominence models. These models are of the (a - c) type of Heasley and Milkey (1976) or perhaps more realistic low-pressure ones of Heasley and Milkey (1978, 1983). The quiescent prominence as seen on the limb is represented by a vertically-standing slab of finite thickness with all model parameters being depth-independent. As basic input parameters we use the set (M, T, p, v_t, y) -see Tab. 1- where M is the total column mass along the line of sight, T is the kinetic temperature, p represents the total

gas pressure and v_t characterizes the mean microturbulent velocity. The prominence plasma is assumed to be composed of hydrogen and helium atoms, the abundance ratio of helium to hydrogen being y = 0.1.

MODEL	M (g/cm^2)	T (°K)	p (dyn/cm^2)	v_t (km/sec)	y
a3	1.2-5	7500	0.065	0	0.1
a5	3.0-5	7500	0.065	0	0.1
LP1	1.2-5	7500	0.010	0	0.1
LP2	3.0-5	7500	0.020	0	0.1
LP3	3.0-5	7500	0.020	6	0.1

Table 1. - Parameters of the prominence models used in this paper.

Since the prominence slab is irradiated symmetrically from both sides by the incident solar radiation, we treat only one half of it. The corresponding second-order boundary conditions for the radiative transfer equation (RTE) are used in the same manner as in Mihalas et al. (1975), but are properly modified for the finite symmetrical slabs (see also Heasley and Mihalas, 1976). The surface boudary condition requires the knowledge of the mean incident radiation field in all lines and continua. For Balmer lines we use the limb-darkened profiles of David (1961), $P\alpha$ $P\beta$ and $B\alpha$ line profiles are taken from Zelenka (1976). All these profiles are subsequently adjusted to limb-darkened continuum level. Disc-center intensities of $L\alpha$ and $L\beta$ lines were obtained by OSO-8 (see, e.g., Vial, 1982a). To obtain the intensity profiles of $L\gamma$ and $L\delta$, we scaled the profile of $L\beta$ by the ratios of total intensities $L\gamma/L\beta$ and $L\delta/L\beta$, respectively. Integrated intensity of $L\beta$ is taken from OSO-8, $L\gamma$ and $L\delta$ from Vernazza and Reeves (1978). In order to obtain the most realistic mean-intensity profiles required in the surface boundary condition, we integrated numerically the above incident intensities, using the geometry and technique as discussed by Heinzel (1983). For all models we use the height 4000 km which corresponds to OSO-8 observations used here for a comparison. By the same procedure we also precomputed all fixed rates for optically thin lines. The continua are treated in two different ways: optically thick Lyman continuum transfer is solved in detail at several frequency points for which we specify the incident radiation temperatures equivalent to intensities measured on OSO-6. For all subordinate continua we simply use one "mean" T_{rad} which defines the corresponding fixed rates (T_{rad} = 5480, 5900, 6200, 6400 K (without dilution) for Balmer, Paschen, Brackett and Pfund continua, respectively).

3. FORMATION OF HYDROGEN LINES WITH PARTIAL REDISTRIBUTION

The laboratory-frame redistribution function (LRF) used in the present computations takes generally the form (Heinzel and Hubeny, 1982)

$$R(\nu', \nu) = \gamma R_i(\nu', \nu) + (1-\gamma) R_{III}(\nu', \nu) \qquad (3.1)$$

with R_i being either R_{II} for the case of the resonance lines or R_V for the lines of subordinate series. While the functions R_{II} and R_V contain certain degree of coherence of the scattering in the line wings, the function R_{III} can be simply replaced by complete redistribution in the observer's frame.

The branching ratio γ is defined as :

$$\gamma = \frac{P_j}{P_j + Q_E} \tag{3.2}$$

where P_j is the total depopulation rate of the upper level j, while Q_E represents the elastic collision rate.
Strictly speaking, Eq. (3.1) has been derived assuming the impact approximation and isolated lines and, therefore, is not applicable to hydrogen lines. However, as demonstrated by Yelnik et al. (1981), the correct ARF (atomic-frame) for hydrogenic $L\alpha$ line is formally the same as that corresponding to LRF (3.1), but the elastic collision rate Q_E is now frequency-dependent. Consequently, the atomic profile function is no longer Lorentzian in the wings and, moreover, the branching ratio is also frequency-dependent (Q_E in (3.1) is replaced by $Q_E(\nu)$).
For $L\beta$ we apply the same procedure with $Q_E(\nu)$ taken from Gouttebroze et al. (1978). For higher members of the Lyman series, we simply use CRD. Moreover, Heinzel (1983) has shown that for quiescent prominences observed on the limb, the subordinate lines exhibit negligible departures from CRD when applying LRF R_V. Anticipating this result, we use in the present computations CRD instead of complicated LRF (3.1) for all subordinate lines.
As a basic procedure to solve the non-LTE transfer problem with PRD we use a combination of an equivalent-two-level-atom approach (ETA) and partial-linearization technique. In the frame of the so-called standard PRD problem (see below), ETA was modified by Hubeny (1985) to account directly for PRD in one line at a time. The resulting source function is

$$S(\nu) = \frac{\overline{J} + \lambda(\overline{R}_{II}(\nu) - \overline{J}) + \eta}{1 + \varepsilon_\nu} \tag{3.3}$$

where $\overline{J}$ is the integrated mean intensity and $\overline{R}_{II}(\nu)$ is the redistribution integral. The parameters η and ε_ν in (3.3) have the similar meaning as in standard ETA (for details see Hubeny, 1985). A very important parameter appearing in Eq. (3.3) is the parameter λ

$$\lambda \simeq \frac{A_{ji}}{P_j} \cdot \frac{P_j}{P_j + Q_E} = \frac{A_{ji}}{P_j} \cdot \gamma \tag{3.4}$$

where A_{ji} is the spontaneous emission rate for the given transition. For strong resonance lines like $L\alpha$ or $L\beta$, λ in form (3.4) reflects the coherence properties of the transition $i \longleftrightarrow j$. Equations (3.3) and (3.4) are valid if all multilevel cross-redistributions lead to a natural population of the upper level j - this is exactly what we call the standard PRD problem, i.e. we consider here no PRD multilevel interlocking.
Simply speaking, γ alone is the branching ratio derived for a two-level-atom, while λ accounts for multilevel processes. From (3.4) we get for $L\alpha$ $\lambda \simeq \gamma$ since $P_2 = A_{21}$. On the other hand, for $L\beta$ we have $P_3 = A_{31} + A_{32}$ so that $\lambda = 0.56\gamma$. Since the ratio γ for both $L\alpha$ and $L\beta$ is nearly equal to unity (for low-density media), the importance of the redistribution term $\overline{R}_{II}(\nu)$ in (3.3) is significantly reduced for $L\beta$ due to the scattering process 2 -> 3 -> 1 which is assumed to contribute to the emission in $L\beta$ as a CRD process.
The numerical procedure for solving the full non-LTE problem is the following: the basic iteration loop uses the linearization scheme as described by Mihalas et al. (1975) to solve simultaneously RTE (by Feautrier method), equations of statistical

equilibrium, particle and charge conservation equations. Hydrostatic equilibrium is treated iteratively, the temperature structure is given from the model. We use 5-level hydrogen atom with continuum and explicitely treat all Lyman lines, Lyman continuum and Hα line. Other transitions are assumed to be optically thin and their radiative rates are fixed by the external radiation field. The linearization loop ensures the global convergence of this highly non-linear problem. Between each two linearization iterations, we perform several ETA iterations, accounting directly for PRD in Lα and Lβ lines. In this way, we obtain fast convergence (within 2 - 3 linearization iterations) in all 50 depths and for all transitions and level populations. We use most important opacity sources for hydrogen spectrum formation in low-density prominences, both ETA and linearization schemes use variable Eddington factors (Auer and Mihalas, 1970) to minimize the computer time. Inelastic collisional rates for hydrogen are taken from Mihalas et al. (1975). The redistribution matrices are used as depth-independent since $P_j >> Q_E$ and the electron and proton densities vary only slowly with depth. On the other hand, the branching ratio $\gamma(\nu)$ is computed for all depths.

4. DISCUSSION OF NUMERICAL RESULTS AND COMPARISON WITH OBSERVATIONS

In Fig. 1 we display typical Lα profiles for both PRD and CRD approaches (for the model LP1).
Drastic differences between CRD and PRD profiles can be explained in the following manner. Around line center, PRD behaves similarly as CRD and the emergent radiation is saturated at the level of diluted incident chromospheric intensity. However, when the scattering takes place in the near wings, we can observe an interesting effect:

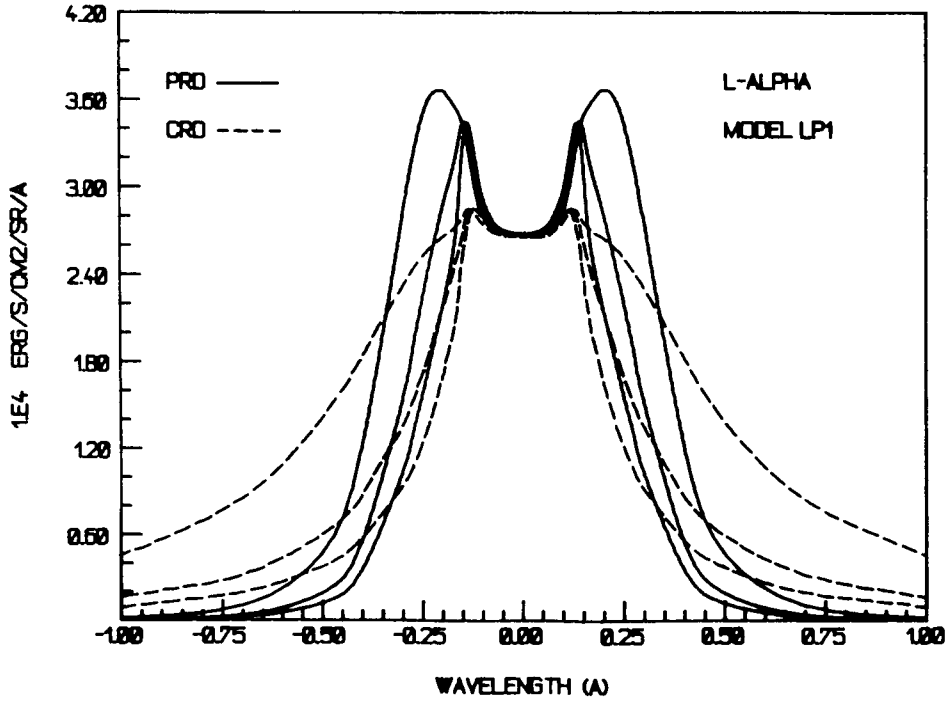

Fig. 1 - Lα intensities emergent from a prominence slab (model LP1). Both PRD (-) and CRD (---) profiles are displayed for three outgoing angles with μ = 1., 0.6 and 0.2 (broader profiles correspond to lower values of μ).

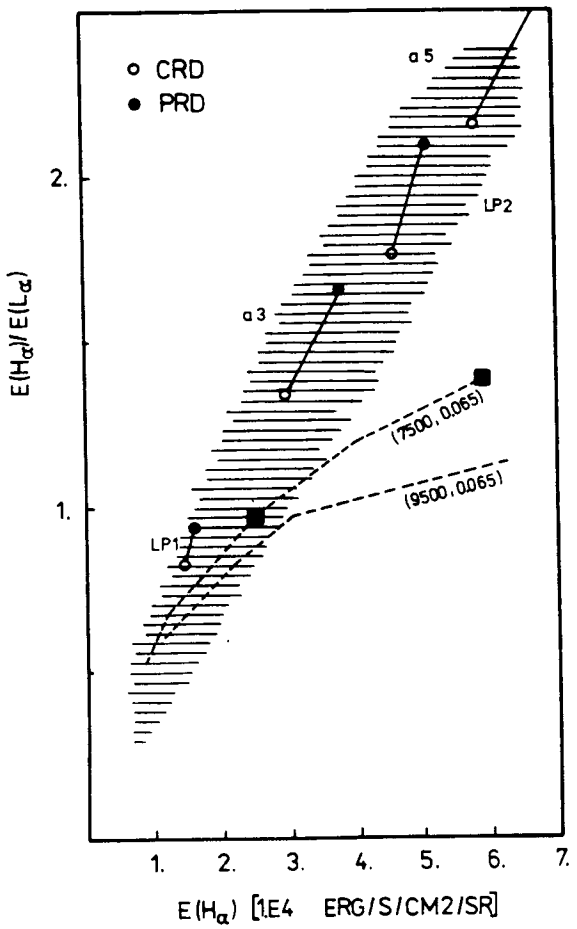

for CRD, the photons absorbed in this region can freely diffuse into the wings which become broad and intense; PRD is, on the other hand, represented by partially-coherent scattering in the wings so that the incident chromospheric Lα peaks (centered at $\Delta\lambda \approx \pm 0.2$ Å) are partly "reproduced" for the PRD case. The photons absorbed in the core or in the near wings cannot freely penetrate into the wings as in the CRD case and, as a consequence, far-wing intensities are sufficiently below the CRD values. Very low PRD wings follow from the well-known behaviour of the redistribution function R_{II}.

Partial reproduction of the strong incident Lα peaks has the following consequences. First, due to quasi-coherent penetration of these peak photons into the slab center, we arrive at higher excitation of hydrogen, i.e. the populations of the excited levels are higher for PRD. As a consequence, the lines of subordinate series are more intense for PRD than for CRD, which is demonstrated for Hα line in Fig. 2.

In this figure, Lα integrated intensities are nearly the same for both PRD and CRD (for PRD, the low intensities in the far wings are compensated by the two peaks), but Hα is shifted in PRD case. In this way we can also explain the results obtained by

Fig. 2 - Dependence of the ratio E(Hα)/E(Lα) on E(Hα), E being the integrated intensity in units ergs s^{-1} cm^{-2} sr^{-1}. Hatched region contains the observed ratios taken from Heinzel and Vial (1983), dashed lines correspond to CRD intensity-ratios as obtained by Heasley and Milkey (1976) for the models indicated in parentheses (labeled by kinetic temperature and total gas pressure). Our theoretical ratios for models a3 and a5 are to be compared with squares on the dashed curve (7500, 0.065). Our CRD (o) and PRD (•) computations are presented for $\mu = 1$.

Milkey et al. (1979): their CRD intensity ratios are shown in Fig. 2 as two dashed lines, a1 - a5 models lie on the curve (7500, 0.065). For models a4 - a5, this curve is significantly below the (hatched) region of observed values as taken from Heinzel and Vial (1983) - this discrepancy is caused probably by adopting unrealistic incident Lα radiation field. The theoretical Lα profiles of Milkey et al. (1979) exhibit only the second PRD-feature, i.e. the low wing intensities. These authors obtained no difference between CRD and PRD for the line core and near wings and, subsequently, their integrated Lα intensities are a factor two lower for PRD as compared with CRD which leads to an apparent agreement with Skylab data. Furthermore, we note that LP1 is the model with lower M and, therefore, for $\mu = 1.$ and 0.6 the incident peak is not fully reproduced due to lower optical thickness of Lα (see Fig. 1). However, for thicker models like LP2 (Fig. 3), LP3 or a5, the incident peak is nicely reproduced and its position agrees well with that for the original peak. It seems that the observed Lα peak-to-peak distance (PTPD) in quiescent

prominences is simply a measure of partially-coherent reproduction of the incident chromospheric peaks and the actual value of PTPD depends on the coherence ratio λ and on the total opacity in Lα.
Finally, PRD leads also to higher electron densities inside the slab, simply due to higher excitation of the second level which controls the photoionization by the Balmer continuum.
For a direct comparison with OSO-8 observations (Vial, 1982a) we used the model LP2.

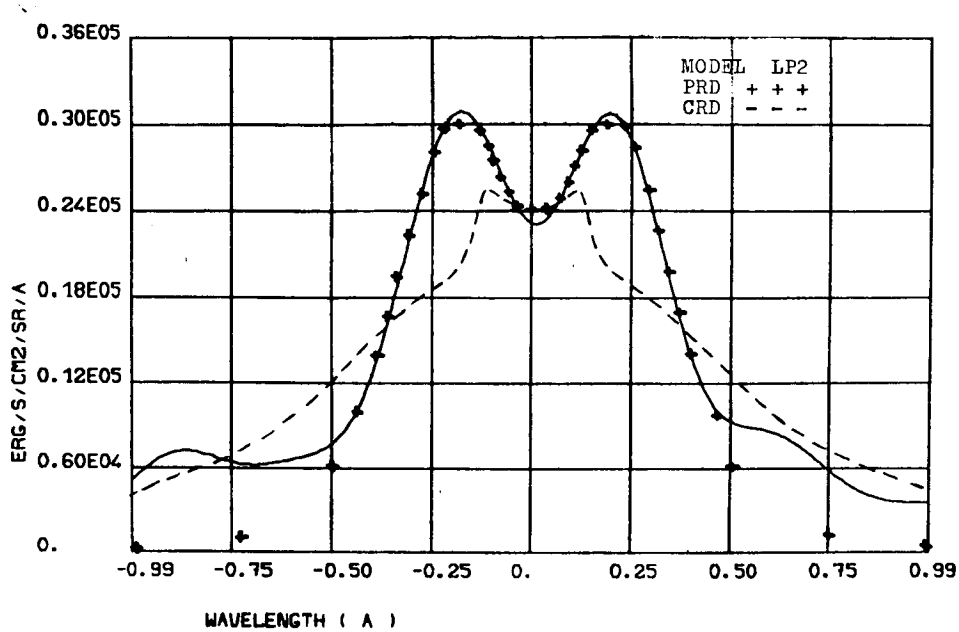

Fig. 3 - Comparison of the observed Lα profile (full line) with theoretical PRD and CRD intensities for model LP2 (μ = 0.6). For details and discussion see the text.

In Fig. 3 we display the observed Lα profile, together with corresponding theoretical PRD and CRD profiles. PRD profile has been smoothed to account schematically for the finite spectrometer resolution (0.02 A) and for small line-of-sight velocities of the order of 5 km/s (see Jensen, 1982). While CRD profile is in no case capable of explaining the observed shape, our PRD Lα profile leads to a reasonable fit. However, there are certain differencies to be discussed. First, the difference in the central dip can be due to either small inaccuracies in the geocoronal-absorption removing, or simply to inappropriate value of the incident radiation used in the computations. Secondly, the observed peaks are somewhat higher than computed. In fact, for thicker models like LP2 we arrived at rather flat peaks and these can be slightly modified when the deconvolution procedure is applied (this is also valid for the flat core). Finally, a wavelike character of the far wings is due to deconvolution so that we can rely on the intensities up to approximately $\pm$ 0.5 A from the line center. As we have found from the computations, the central intensity of Lα is determined mainly by the value of the diluted incident radiation and is insensitive to variations of the model parameters. On the other hand, the peak value is somewhat lowered for non-zero v_t (model LP3).
The profile parameters, corresponding to Fig. 3, are summarized in Table 2. We see

that our PRD values reproduce quite well the observations, possibly except for the total intensity corrected for the filling factor (note that the actual observed value of E can be lower with respect to data-reduction effects discussed above). The 2D total intensity is too low even when CRD is used. Note also a satisfactory agreement between Hα intensities. Finally, the electron density as obtained for LP2 model ($n_e = 7 \times 10^9$ cm^{-3}) is in good agreement with the values recently obtained from polarimetric observations (Bommier, present volume). The geometrical thickness of the prominence is somewhat large - 11 500 km -, but this corresponds to a low gas pressure 0.02 dyn/cm^2.

	Lα				Lβ			Hα		
PARAMETERS	LP2 PRD	LP2 CRD	2D CRD	OBS. FPO	LP2 PRD	LP2 CRD	OBS. FPO	LP2 PRD	LP2 CRD	OBS.
FWHM (A)	0.76			0.74	0.26	0.23	0.61			
PTPD (A)	0.37	0.23	0.32	0.37	(no reversal)		0.33			
I(peak)/I_o	1.25	1.06	1.3	1.33	(no reversal)		1.85			
E_1(x10^4)	2.70	3.03	1.61	2.84	0.007	0.005	0.044	7.51	6.76	5.-9.
E_2(x10^4)				3.55			0.055			

PTPD - peak-to-peak distance - I_o - central intensity (prominence)
E_1 (ergs s^{-1} cm^{-2} sr^{-1}) - integrated intensity
E_2 - as E_1 but corrected for filling factor (see Vial, 1982a)

Table 2.

Comparison of basic profile parameters of Lα , Lβ and Hα . LP2 is the model from Table 1, 2D model corresponds to the computations of Vial (1982b), FPO means "first part of orbit" (see Vial, 1982a). Hα intensity was estimated using OSO-8 CaII intensities and the relation between CaII and Hα as given by Stellmacher (1979). Lα parameters correspond to the profiles in Fig. 3. Theoretical Lα profiles for the model LP2 have been corrected for the actual value of the calibration disc-center intensity (6.5 x 10^4 ergs s^{-1} cm^{-2} sr^{-1}), for LP2 we used the values for $\mu = 0.6$.

As we have found during the course of our investigation, Lβ line presents, on the other hand, a complicated and so far unresolved problem. Looking at Table 2, we see immediately that the basic Lβ profile-parameters differ significantly from the observed ones and, moreover, the theoretical integrated intensity is also a factor 5 - 10 lower than the observed value (for both CRD and PRD). This surprising result needs further verifications and more sophisticated calculations are to be done to resolve this discrepancy.
Our knowledge of the Lβ radiation field inside the prominence is also essential for estimating the degree of Hα line polarization (from which we can deduce the magnetic-field topology via the Hanle effect -see Bommier, present volume-) and, therefore, PRD-interlocking as well as various multidimensional effects are to be properly accounted for in the future computations.

5. CONCLUSIONS

We have demonstrated the most important effects of PRD in the formation of hydrogen Lα line in quiescent prominences. Except for the well-known lowering of the far wings as compared to CRD, we have found a new PRD feature for Lα prominence line: strong peaks of the incident solar radiation are partly reproduced due to quasi-coherent scattering in the near wings of Lα and, as a consequence, we obtain typical prominence Lα profiles with significant central reversal and PTPD comparable to the solar one. All features we have found are actually observed as our comparison with OSO-8 data shows. However, for Lβ line we arrived at a substantial discrepancy between the theoretical and observed intensities. Having estimated the differential PRD effects for Lα , future computations should try to establish the proper interplay between PRD and multidimensional radiation-transport influences on the prominence spectral diagnostics. Our present report should serve as a starting point in developing more sophisticated non-LTE techniques which will be capable of explaining new data from UVSP/SMM or other planned space experiments.

ACKNOWLEDGEMENTS

One of us (P.H.) highly appreciates the possibility to stay at LPSP in 1984, where this work was originated. P.H. and J.C.V. would like to thank NASA for its financial support which enabled them to present this report during the CPP-workshop. All numerical computations were performed using the facilities of the Ondrejov Observatory Computing Center and the Cray-1 computer of the "Centre de calcul Vectoriel pour la Recherche".

REFERENCES

Auer, L.H., Mihalas, D.: 1970, M.N.R.A.S. 149, 60.
David, K.H.: 1961, Z. für Astrophys. 53, 37.
Gouttebroze, P., Lemaire, P., Vial, J.C., Artzner, G.: 1978, Astrophys. J. 225,655.
Heasley, J.N., Mihalas, D.: 1976, Astrophys. J. 205, 273.
Heasley, J.N., Milkey, R.W.: 1976, Astrophys. J. 210, 827.
Heasley, J.N., Milkey, R.W.: 1978, Astrophys. J. 221, 677.
Heasley, J.N., Milkey, R.W.: 1983, Astrophys. J. 268, 398.
Heinzel, P.: 1983, Bull. Astron. Inst. Czechosl. 34, 1.
Heinzel, P., Hubeny, I.: 1982, J. Quant. Spectrosc. Radiat. Transfer 27, 1.
Heinzel, P., Vial, J.C.: 1983, Astron. Astrophys. 121, 155.
Hubeny, I.: 1985, Bull. Astron. Inst. Czechosl. 36, 1.
Jensen, E.: 1982, Sol. Phys. 77, 109.
Mihalas, D., Heasley, J.N., Auer, L.H.: 1975, NCAR Technical Note NCAR-TN/STR-104, NCAR, Boulder.
Mihalas, D., Auer, L.H., Mihalas, B.R.: 1978, Astrophys. J. 220, 1001.
Milkey, R.W., Heasley, J.N., Schmahl, E.J., Engvold, O.: 1979, in Physics of Solar. Prominences, IAU Coll. 44, Eds. Jensen, E., Maltby, P., Orrall, F., Inst. Theor. Astrophys., Oslo, 53.
Stellmacher, G.: 1979, Sol. Phys. 61, 61.
Vernazza, J.E., Reeves, E.M.: 1978, Astrophys. J. Suppl. 30, 1.
Vial, J.C.: 1982a, Astrophys. J. 253, 330.
Vial, J.C.: 1982b, Astrophys. J. 254, 780.
Yelnik, J.B., Burnett, K., Cooper, J., Ballagh, R.J., Voslamber, D.: 1981, Astrophys. J. 248, 705.
Zelenka, A.: 1976, Astron. Astrophys. 48, 75.